Molecular Medicine

The JAK–STAT Pathway Is Critical in Ventilator-Induced Diaphragm Dysfunction

Huibin Tang,[1,2] Ira J Smith,[3] Sabah NA Hussain,[4] Peter Goldberg,[4] Myung Lee,[1,2] Sista Sugiarto,[1,2] Guillermo L Godinez,[3] Baljit K Singh,[3] Donald G Payan,[3] Thomas A Rando,[5,6] Todd M Kinsella,[3] and Joseph B Shrager[1,2]

[1]Division of Thoracic Surgery, Department of Cardiothoracic Surgery, Stanford University School of Medicine, Stanford, California, United States of America; [2]Veterans Administration Palo Alto Healthcare System, Palo Alto, California, United States of America; [3]Rigel Pharmaceuticals, South San Francisco, California, United States of America; [4]Critical Care Division, Royal Victoria Hospital, Montreal, Quebec, Canada; [5]Department of Neurology and Neurological Science, Stanford University School of Medicine, Stanford, California, United States of America; and [6]Neurology Service, Veterans Administration Palo Alto Healthcare System, Palo Alto, California, United States of America

Mechanical ventilation (MV) is one of the lynchpins of modern intensive-care medicine and is life saving in many critically ill patients. Continuous ventilator support, however, results in ventilation-induced diaphragm dysfunction (VIDD) that likely prolongs patients' need for MV and thereby leads to major associated complications and avoidable intensive care unit (ICU) deaths. Oxidative stress is a key pathogenic event in the development of VIDD, but its regulation remains largely undefined. We report here that the JAK–STAT pathway is activated in MV in the human diaphragm, as evidenced by significantly increased phosphorylation of JAK and STAT. Blockage of the JAK–STAT pathway by a JAK inhibitor in a rat MV model prevents diaphragm muscle contractile dysfunction (by ~85%, $p < 0.01$). We further demonstrate that activated STAT3 compromises mitochondrial function and induces oxidative stress *in vivo*, and, interestingly, that oxidative stress also activates JAK–STAT. Inhibition of JAK–STAT prevents oxidative stress-induced protein oxidation and polyubiquitination and recovers mitochondrial function in cultured muscle cells. Therefore, in ventilated diaphragm muscle, activation of JAK–STAT is critical in regulating oxidative stress and is thereby central to the downstream pathogenesis of clinical VIDD. These findings establish the molecular basis for the therapeutic promise of JAK–STAT inhibitors in ventilated ICU patients.

Online address: http://www.molmed.org
doi: 10.2119/molmed.2014.00049

INTRODUCTION

Mechanical ventilation (MV) is an important component of modern medical practice which allows support of breathing in the intensive care unit (ICU) and during surgery requiring general anesthesia. Many patients, however, fail initial weaning from the ventilator and enter the difficult realm of prolonged ventilation. Patients who develop this ventilator dependence, though a diverse group, share the common underlying problem of substantial dysfunction of the major inspiratory muscle, the diaphragm (1–8). The development of ventilator-induced diaphragm dysfunction (VIDD) appears to be a major underlying cause of prolonged ventilator-dependence with its attendant dramatic increase in morbidity and mortality (9–14).

The pathogenesis of VIDD includes both atrophy of diaphragmatic myofibers and loss of diaphragmatic contractile function (that is, specific force) unrelated to atrophy (15–17). In previous studies, MV with diaphragm inactivity has been shown to elicit significant dysfunction and/or atrophy of myofibers in the diaphragm of humans (18–21), rats (22), mice (23–25), rabbits (26) and piglets (27). With regard to the atrophy, several proteolytic events, such as activation of the ubiquitin proteasome system (UPS) (28–30), autophagy (24,25,31) and apoptosis (32–35), and upregulation of calpain (36), have been demonstrated in MV models. We and others have re-

Address correspondence to *Joseph B Shrager, Division of Thoracic Surgery, Department of Cardiothoracic Surgery, Stanford University School of Medicine, 2nd floor, Falk building, 300 Pasteur Dr., Stanford, CA 94305-5407. Phone: 650-721-2086; Fax: 650-724-6259; E-mail: shrager@stanford.edu; and Todd Kinsella, Rigel Pharmaceuticals, Inc., 1180 Veterans Blvd., South San Francisco, CA 94080. Phone: 650-624-1285; E-mail: tkinsella@rigel.com.*
Submitted March 12, 2014; Accepted for publication September 30, 2014; Epub (www.molmed.org) ahead of print September 30, 2014.

ported that oxidative stress is induced in MV diaphragm (35,37,38) and that the elevated mitochondrial oxidative stress (MOS) in MV human diaphragm appears to be a key upstream inducer of these proteolytic events (35).

In addition to promoting protein turnover, MOS could impact specific force as well in at least two ways. MOS generates free radicals that may directly oxidize muscle proteins, altering their structure and function, including changes to myofilament structure, crossbridge kinetics and/or a reduction of the calcium sensitivity of myofilaments (39–42). Secondly, MOS is able to induce a metabolic switch, a reduction in mitochondrial oxidative phosphorylation and an increase in glycolysis (43–46), which may lead to reduced overall energy supply to the muscle. Since reduction of specific force occurs prior to the presence of muscle atrophy in the ventilated human diaphragm (20,23), this component of VIDD may account for the earliest and perhaps most critical phase of the process. Therefore, understanding the basis of MOS generation in the MV diaphragm would be likely to identify targets that could be used to impact the most clinically important phase of VIDD.

The JAK–STAT pathway, consisting of Janus kinase (JAK) and signal transducer and activator of transactivation (STAT), is a signaling cascade that can be activated by cytokines, hormones and growth factors via ligand-receptor interactions. The consequentially activated JAK kinase can further phosphorylate STAT proteins, and the latter usually form dimers, translocate to the nucleus and transcriptionally activate genes. In a previous study, we found that *STAT3* gene expression level was upregulated in ventilated human diaphragm and that this upregulation was linked to the activation of mitochondrial apoptosis (35). It also was recently reported that overexpression of STAT3 can lead to skeletal muscle atrophy (47). In addition, oxidative stress has been shown to activate the JAK–STAT pathway *in vitro* (48). Therefore, it is reasonable to speculate that MV-induced oxidative stress elevates STAT3 and thereby contributes to the muscle atrophy component of VIDD. However, whether and how the JAK–STAT pathway contributes to the reduction in diaphragm muscle specific force associated with prolonged MV remains unknown.

In the current study, we report that JAK and STAT are significantly phosphorylated/activated in both human and rat diaphragms subjected to MV. Blockade of the JAK–STAT pathway in ventilated rats dramatically prevents the loss of contractile function in their diaphragms. Overactivation of JAK–STAT induces oxidative stress in skeletal muscle *in vivo*, with increased protein oxidation and reduction in mitochondrial membrane potential. Interestingly, JAK–STAT also can be activated by oxidative stress, and inhibition of JAK or STAT can suppress H_2O_2-induced oxidative stress. Together, these findings strongly suggest that the regulation of oxidative stress via activation of JAK–STAT is crucial in the development of VIDD. This work renders the JAK–STAT pathway an optimal target for a drug to prevent VIDD.

MATERIALS AND METHODS

Human Samples

The human samples were collected as described in detail previously at the University of Pennsylvania, Philadelphia, USA (30) and the Royal Victoria Hospital, Montreal, Quebec, Canada (31). Control diaphragm muscle biopsies were taken from patients 69.4 ± 4.7 years old (range 63 to 83 years old) with body mass index (BMI) 24.1 ± 0.52 kg/m^2 (range 23.3 to 26.6 kg/m^2). The ventilation time for the controls was 1.21 ± 0.1 h (range 1 to 1.5 h). The MV diaphragm samples were taken from patients 58.2 ± 4.6 years old (range 41 to 75 years), mean BMI 27.1 ± 1.77 kg/m^2 (range 23 to 31 kg/m^2). The average MV time for these patients was 49 ± 8.6 h (range 12 to 74 h). Nonrespiratory control muscles from these control and MV patients were taken from the quadriceps muscle, as described previously (31,35).

Mechanical Ventilation of Rats and Measurement of Diaphragm Contractile Function

Animal protocols were approved by the Institutional Animal Care and Use Committees of Rigel Pharmaceuticals, Inc. All animal experiments were carried out according to recommendations in *Guide for the Care and Use of Laboratory Animals* (eighth edition) (49). All surgical procedures were performed using aseptic techniques. Animals (Sprague Dawley rats, 270 ± 10g) were anesthetized to a surgical plane of anesthesia with isoflurane (2% to 4%) and a tracheotomy was performed. Rats were maintained on MV with isoflurane for 18 h using a volume-driven small-animal ventilator (CWE, Ardmore, PA, USA). Tidal volume was set at 0.7 mL/100 g body weight, respiratory rate was 80/minute. A carotid artery catheter was utilized to monitor blood pressure and to collect arterial blood samples. JAK inhibitor or control vehicle were delivered continuously through a jugular vein cannula. Heart rate was monitored throughout the study using ECG needle electrodes, and body temperature was maintained at 37°C by a rectal temperature probe connected to a Homeothermic Blanket System. Body fluid homeostasis was maintained via subcutaneous administration of 1.7 mL/kg body weight/2.5 h saline. To reduce airway secretions, glycopyrrolate (0.04 mg/kg) was administered subcutaneously every 2.5 h. After 18 h continuous MV, the rats were euthanized and diaphragms were collected and either used immediately for contractile function studies or snap frozen in liquid nitrogen for biochemical assays stored at –80°C.

Diaphragm contractile function was determined using diaphragm strips maintained *ex vivo*, as described previously (38). Briefly, upon completion of the study, the entire diaphragm was removed and transferred to a dissecting dish containing Krebs-Hensleit physio-

logical solution aerated with 95% O_2 to 5% CO_2 gas. A muscle strip was dissected from the midcostal region of the diaphragm, which included a portion of the central tendon and ribcage. The strip was mounted vertically using serrated jaw tissue clamps, with one end fixed to an isometric force transducer on a tissue organ bath system 750 (DMT, Ann Arbor, MI, USA), and immersed in the same solution. After a 15-min equilibration, diaphragm strips were stimulated with a S88X Pulse Stimulator (Grass Technologies, Warwick, RI, USA), and platinum wire electrodes (Radnotti, Monrovia, CA, USA). Contractile measurements were taken at the optimal muscle length (Lo), the length at which maximal force is obtained. Lo was determined by stimulating the muscle at a supramaximal voltage, and systematically adjusting the muscle length. The force–frequency relationship was assessed by stimulating each strip supramaximally with 8-V pulses, with a train duration of 500 ms, at 15–160 Hz. Contractions were separated by a two-minute recovery period. Diaphragm force production was normalized as specific force based on muscle cross-sectional area (CSA). Total muscle CSA at right angles to the long axis was determined by the following calculation: total muscle CSA (mm^2) = [muscle mass/(fiber length × 1.056)], where 1.056 is the density of muscle (in g/cm^3). Fiber length was expressed in centimeters measured at Lo.

Reagents and Plasmids

A pan-JAK inhibitor 1 (JAK I) and STAT3 inhibitor (stattic) were purchased from EMD Millipore (Billerica, MA, USA). The JAK inhibitors, R545 and R548, were generated at Rigel Pharmaceuticals. Both are potent JAK inhibitors, with an inhibitory effect over JAK1/3 at 0.03 nmol/L and JAK2 at 1.1 nmol/L (Supplementary Table S1). H_2O_2 was purchased from Sigma-Aldrich (St. Louis, MO, USA). Lipofectamine 2000 was purchased from Invitrogen/Life Technologies/Thermo Fisher Scientific (Waltham, MA, USA). pcDNA3.1–STAT3C was constructed in lab by digestion of an EF1-STAT3C-ubc-GFP construct (Addgene Inc., Cambridge, MA, USA) with Hind3 and then ligated into pcDNA3.1 vector at the Hind3 site. The final construct was sequenced for validation. Prk5-JAK2V617F was a gift from Lawrence Argestinger (University of Michigan) with the permission of James Ihle (Saint Jude Children's Research Hospital). pcs2-GFP and pcs2-bGal plasmids were from David Turner and Daniel Goldman (University of Michigan).

Cell Culture and Transfection

Plasmids were transfected into HEK293 cells with lipofectamine 2000. Three days later, ATP content or luciferase assays were performed. The co-transfected pcs2-β-Gal was used for normalization via β-Gal assay according to standard procedures.

Gene electroporation was performed as described previously (44). Briefly, 20 μg of control plasmid (pcDNA3 vector) or 20 μg of pcDNA3-STAT3C plasmid was mixed with 2 μg pcs2-GFP plasmid, respectively, and injected into mouse tibialis anterior (TA) muscles, immediately followed by 8 pulses of electrical shocks at 140V/cm of 60-ms duration with an interval of 100 ms, delivered by ECM830 (Harvard Apparatus, Holliston, MA, USA) square wave electroporation system. After 10 d, the TA muscles were collected, and GFP+ fibers (~25% of the muscle) were isolated with fine forceps under the fluorescent dissecting scope. The high ratio (10 to 1) of the plasmids containing the gene of interest to the plasmid containing the GFP reporter ensures that nearly all GFP+ fibers express the gene of interest. Total protein was extracted from these GFP+ fibers by RIPA buffer and then subjected to Western blot analysis.

JC1 Mitochondrial Membrane Potential Assay

Mitochondrial membrane potential assay was performed with the JC-1 reagent (Cayman Chemical Company, Ann Arbor, MI, USA). The JC-1 reagent was diluted 1:10 in JC-1 assay buffer to prepare the JC-1 staining solution. Ten microliter of staining solution was added to the 100 μL of culture media, incubating at 37°C for 30 min. The plate was centrifuged (400*g*, 5 min) at room temperature, and the supernatant was removed. After being washed three times with an assay buffer, cells were then analyzed with a SpectraMax M2e Multi-Mode Microplate Reader (Molecular Devices LLC, Sunnyvale, CA, USA) for live cells (excitation/emission at 560/595 nm) and dead cells (excitation/emission at 485/535 nm).

ATP Content Measurement

ATP content in cells was measured with a Biovision ATP assay kit according to the supplier's instructions. Briefly, cells were lysed in 200 μL ATP assay buffer provided by the manufacturer (BioVision, San Diego, CA, USA). The samples were then centrifuged at 20,183*g* for 15 min at 4° to pellet insoluble materials. Supernatants were collected into a fresh set of tubes for the assay. Fifty microliter of the reaction mix was added to 50 μL of lysate to start the ATP reaction. The optical density (OD) 570 nm was measured at 10 to 20 min intervals and the concentrations were calculated using the standards provided by the manufacturer. The ATP concentrations were then normalized to total protein concentrations.

Immunostaining and Western Blotting

Cultured C2C12 muscle cells on slides were fixed with 2% PFA for 30 min, and the immunostaining was performed by standard procedures. Anti-STAT3 antibody was purchased from Cell Signaling Technology (Danvers, MA, USA); and Alexa555-conjugated anti-rabbit secondary antibody and Alexa488-WGA were purchased from Invitrogen/Life Technologies/Thermo Fisher Scientific. Mounted cells were then imaged by confocal microscopy (Zeiss, Jena, Germany).

Protein expression levels were detected by Western blot analysis following standard procedures. Primary antibodies, anti-DNP (dinitrophenol) and 4-HNE (4-hydroxy-2-nonenal), were purchased

from Abcam (Cambridge, England); primary antibody anti-nitrotyrosine was purchased from EMD Millipore. The rest of the antibodies used in this study were purchased from Cell Signaling Technology. The phosphorylation sites specifically recognized by these antibodies are pJAK1-tyr1022/1023, pJAK2-tyr1007/1008, pJAK3-tyr980/981, pSTAT5-tyr694 and pSTAT3-tyr705.

Gene Profiling, Quantitative PCR

Gene profiling was performed as described (35). mRNA expression levels were detected by real-time PCR by standard procedures. The primers used are listed in Supplementary Table S2.

Statistical Analyses

Quantitation of gray density was performed with ImageJ software (National Institutes of Health, Bethesda, MD, USA; http://imagej.nih.gov/ij). One-way analysis of variance (ANOVA) was used to determine the significant changes when there were more than three groups for comparison, followed by Tukey *post hoc* test. Student *t* test was used to evaluate the significance while comparing two groups in this study. A level of $p < 0.05$, indicated by and asterisk (*) in figures, was considered significant.

RESULTS

The JAK–STAT Signaling Pathway Is Activated in MV Human Diaphragm

To understand the molecular pathogenesis of VIDD, we began by analyzing gene profiling data from control (MV <2 h) and ventilated (MV >18 h) human diaphragm samples. With the DAVID bioinformatic tool, we found that at least 15 signaling pathways are significantly ($P < 0.05$) altered in ventilated human diaphragm, including those linked to previous observations in ventilated diaphragm, such as the toll-like receptor (24), apoptosis (35), glycolysis (44), calcium (33) and adipocytokine signaling pathways (50). However, several novel pathways not previously reported, including JAK–STAT, Wnt, MAPK, TGF-β and the insulin/mTOR signaling pathway, also were identified (Figure 1A and Supplementary Table S3). The JAK–STAT signaling pathway is among the most significantly ($p < 0.0001$) altered KEGG pathways (see Figure 1A and Supplementary Table S3), as evidenced by increased expression of both upstream inducer genes, such as *IL6* and *IL24*, and the downstream target gene *SOCS3* (Figure 1B). We validated the increased expression of these genes by quantitative PCR (Figure 1C).

Since the increased expression of IL6 and IL24 can lead to activation of the JAK–STAT signaling pathway by inducing the phosphorylation of JAK and STAT proteins, we examined the phosphorylation levels of JAK and STAT. We find that the phosphorylated forms of JAK1 (pJAK1-Y1022/1023), JAK2 (pJAK2-Y1007), JAK3 (pJAK3-Y980/981), STAT3 (pSTAT3-Y705) and STAT5 (pSTAT5-Y694) all are significantly upregulated in human ventilated diaphragm (Figure 1D), ranging from two-fold to 3.5-fold. Since phosphorylated STAT3 forms dimers and translocates into nuclei to regulate gene expression, we examined the subcellular distribution of STAT3 in MV diaphragm by immunostaining. These results indicate that STAT3 protein is indeed enriched in diaphragmatic myonuclei following MV (Figure 1E).

The activation of STAT appears to be diaphragm-specific, since it is not activated in the quadriceps muscles of the ventilated patients (Figure 1F). This indicates that the activation of STAT3 in diaphragm muscle is unlikely to be occurring through systemic factors.

Blockade of the JAK–STAT Pathway with a JAK Inhibitor Substantially Prevents Diaphragm Muscle Contractile Dysfunction in a Rat MV Model

To investigate the functional significance of the activated JAK–STAT signaling pathway in MV diaphragm, we employed a JAK inhibitor to block the activation of JAK–STAT in a rat MV model. MV was performed on adult SD rats for 18 h and the JAK inhibitor (R545) was delivered by continuous intravenous infusion. As in MV human diaphragm, the phosphorylation level of STAT3 (Y705) is significantly induced in MV rat diaphragm (Figure 2A). Delivery of the JAK inhibitor completely blocks the increase in STAT3 phosphorylation (see Figure 2A).

Although diaphragm muscle fiber size is in fact reduced in this model of MV rat diaphragm (51), the specific force (that is, the maximum contractile force normalized to fiber size measured with stimulated diaphragm strips), is even more dramatically reduced (down to ~50% of control). Diaphragm strips also appear somewhat more fatigable following MV, although the major difference between control and MV diaphragm strips is clearly the difference in specific force, which remains significant up to the 4-min point during a fatiguing protocol. JAK inhibitor treatment prevents the loss of maximal diaphragm force-generating capacity (median rescue of ~85% relative to untreated MV rat diaphragm at 100 Hz; $p = 0.0028$) (Figures 2B–D).

These data indicate that activation of JAK–STAT is necessary for the reduction in specific force, and thereby the development of VIDD.

Enhanced Activity of JAK–STAT Induces Oxidative Stress *In Vitro* and *In Vivo*

Although the above data indicate that JAK–STAT might be critical in the development of VIDD, it remains unclear from this data which pathogenic changes this signaling pathway support that lead to VIDD. Since oxidative stress is known to be activated in both rat and human MV diaphragm (35,37,38) and is a key pathological event in directing the evolution of VIDD (35), we hypothesized that activated JAK–STAT may reduce the specific force in diaphragm muscle by inducing oxidative stress in this disease process.

To test this hypothesis, we first examined if activation of JAK–STAT is able to induce oxidative stress. We transfected a plasmid with cDNA encoding a constitutively active STAT3 (STAT3C) cDNA into

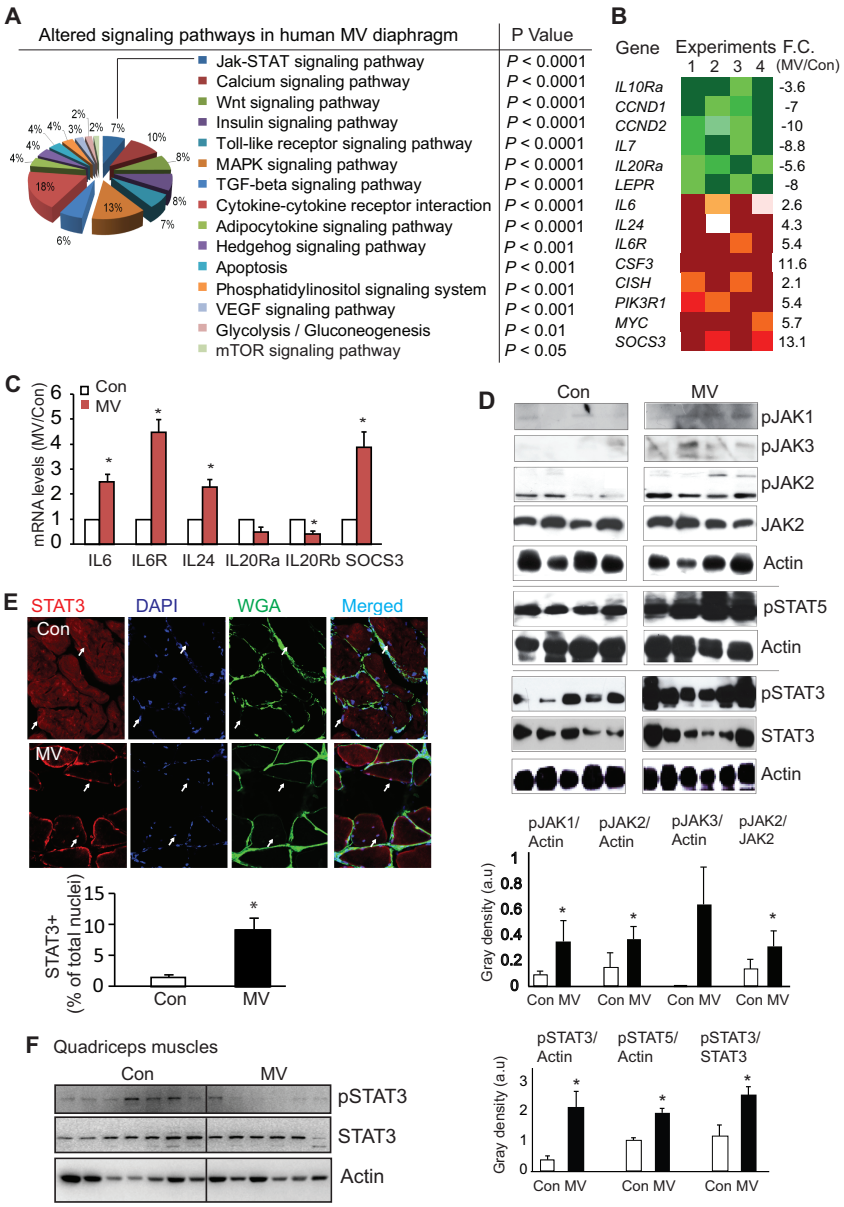

Figure 1. Activated JAK–STAT signaling pathway in MV human diaphragm. (A) Altered signaling pathways in the MV human diaphragm. Altered genes ($p < 0.05$) from microarray analysis of MV versus control diaphragm samples were input into DAVID Bioinformatics analysis. In the pie figure, the percentage indicates the number of genes involved in the specific pathway over the total number of genes involved in all signaling pathways listed. The p value indicates the significance of the altered signaling pathway. Signal pathways with $p < 0.05$ are listed. (B) The mean fold change in MV versus control human diaphragm samples of genes significantly ($p < 0.05$) altered by MV that are involved in the JAK–STAT signaling pathway (n = 4 pairs of samples). The color green in the heat map indicates the reduced expression of genes, while red indicates increased expression. Specific fold changes are indicated in the right column. (C) Quantitative PCR was performed to confirm the altered expression of genes identified by microarray. Human diaphragm muscle samples (Con n = 6, MV n = 8) were examined, $^*p < 0.05$. (D) Activation of the JAK–STAT signaling pathway. Protein extracts from MV and control human diaphragm muscles were subjected to Western blot analysis (n ≥ 4). The two lower bar graphs show the data quantified, with normalization of phosphorylated protein. $^*p < 0.05$. (E) Nuclear enrichment of STAT3 in MV human diaphragm. Human diaphragm muscles were stained with STAT3 (red), DAPI (blue) or WGA (green) to show STAT3, nuclei and cell membrane respectively. Arrows indicate the location of nuclei. The lower panel shows the quantitated data of the STAT3-positive nuclei per total nuclei. n = 4, $^*p < 0.05$. Note that STAT3 is enriched in nuclei in the ventilated but not the control human diaphragms. (F) STAT3 is not activated in nonrespiratory muscles during mechanical ventilation. Protein extracts from human quadriceps muscles from control and MV patients, and subjected to Western blot analysis. Note that there is no induction of phosphorylated STAT3 in quadriceps muscles under MV. F.C., fold changes; Con, control; IL6R, interleukin-6 receptor; IL20Ra, interleukin-20 receptor alpha subunit; IL20Rb, interleukin-20 receptor beta subunit; a.u., arbitrary unit.

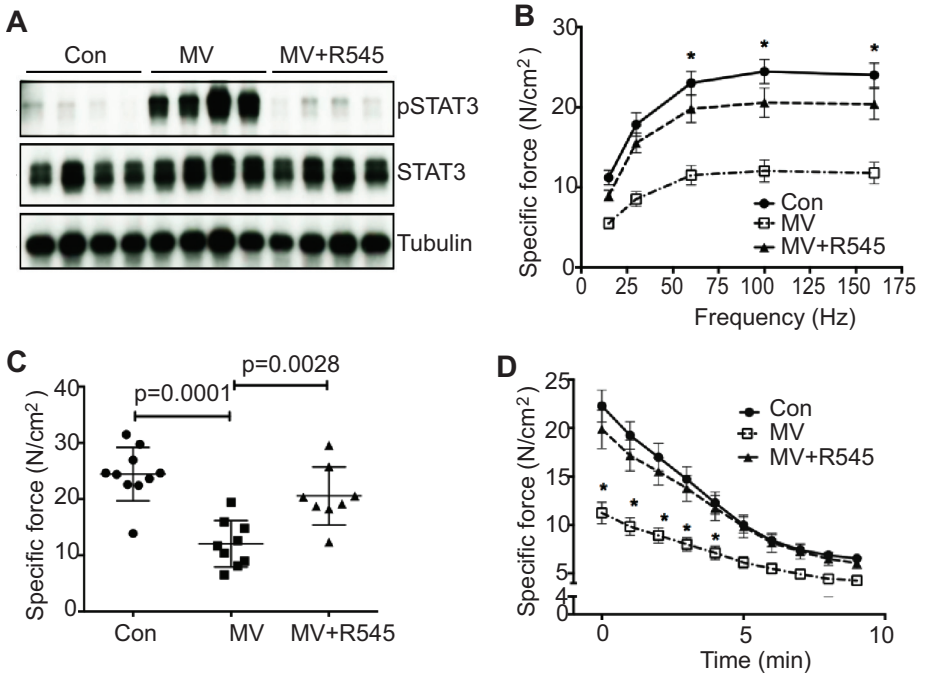

Figure 2. JAK inhibition prevents the reduction of muscle-specific force that occurs in mechanically ventilated rats. (A) Mechanical ventilation induces STAT3 phosphorylation and JAK inhibitor blocks this activation. Control and MV (18 h) rat diaphragm muscles were subjected to Western blot analysis (n = 4 rats per group). (B–D) Treatment with a JAK inhibitor (R545) prevents MV-induced contractile dysfunction. The diaphragms from controls (n = 10) and MV rats treated with the JAK inhibitor (n = 8) or vehicle (n = 9) were analyzed: (B) Diaphragm strip *ex vivo* force–frequency relationship; (C) Specific force generation at 100 Hz; and (D) Fatigue development after 18 h of MV. Con, control.

the mouse tibialis anterior (TA) muscle via electroporation. STAT3C is a mutant form of STAT3, which is constitutively active due to the mutation of alanine (A) 661 to cysteine (C) and asparagine (N) 663 to cysteine (C). After confirming an increased expression of STAT3C in skeletal muscle (Figure 3A), we found that overexpression of STAT3C results in the induction of protein expression of Bcl2l11 (Bim), a modulator of mitochondrial membrane potential and a proapoptotic gene. However, the protein levels of several mitochondrial components, C1 (NDUFB8), C2 (SDHB), C3 (UQCRC2) and C5 (ATP5A), do not show significant change (Figures 3A, B). Overexpression of STAT3C also leads to increased protein oxidation, evidenced by increased abundance of nitrotyrosine and 4-hydroxynonenal (4-HNE) (Figure 3C, D), indicating that the increased STAT3 activity in skeletal muscle does induce oxidative stress. In addition, there is a dramatic induction of muscle protein ubiquitination following overexpression of STAT3C (see Figures 3C, D). Although increased protein oxidation and ubiquitination often are linked to protein degradation and thus contribute to muscle atrophy, it is also possible that these posttranslational modifications affect the contractile function of muscle proteins and thus lead to the reduction in specific force, prior to protein degradation. Together, the increased protein posttranslational modifications appear to link the proteasome-mediated protein degradation and the reduction in specific force that occurs in VIDD to a common regulatory pathway, that is, the JAK–STAT pathway.

Since constitutively active STAT3 increases the expression of Bcl2l11 (Bim) protein, which can alter mitochondrial membrane potential, activated JAK–STAT may affect mitochondrial function. In fact, it has been reported that overexpression of STAT3C reduces mitochondrial membrane potential (52). Here we demonstrate that overexpression of a constitutively active JAK2 reduces mitochondrial membrane potential, shown by the reduced JC1 index with overexpression (Figure 3E).

We also examined the transcriptional regulation of gene expression by STAT3 in cultured cells. Overexpression of STAT3C leads to induction of SOCS3 and Bcl2l11 (Bim) (Figure 3F). Concomitantly, UCP2, a mitochondrial transporter protein that creates a proton leak across the inner mitochondrial membrane, thereby reducing the efficiency of energy production by uncoupling oxidative phosphorylation from ATP synthesis, is induced by STAT3C (see Figure 3F). On the other hand, Cox5b, a nuclear-encoded mitochondrial gene that functions in electron transport, is significantly downregulated by STAT3C (see Figure 3F). This profile of gene expression is thus consistent with the functional decline in mitochondria induced by activated STAT3.

Consistent with the STAT3-induced changes in gene expression, MV leads to suppression of the mRNA expression of NDUFS3 and UQCRC2 in rat diaphragm muscle, and the pan-JAK inhibitor rescues the suppression of NDUFS3 (Supplementary Figure S1). This clearly indicates a role of JAK–STAT in regulating the expression of these genes that are relevant to mitochondrial function.

JAK–STAT Is Both Activated by H_2O_2-Induced Oxidative Stress and Is Essential for the Evolution of Oxidative Stress

The above work suggests that MV-activated JAK–STAT leads to VIDD in part by inducing oxidative stress. However, how JAK–STAT is activated in the MV diaphragm remains unclear. We developed an *in vitro* oxidative stress model in cultured muscle cells based upon H_2O_2 treatment. We find that H_2O_2-induced oxidative stress activates the JAK–STAT signaling pathway in muscle cells, as evidenced by the increased

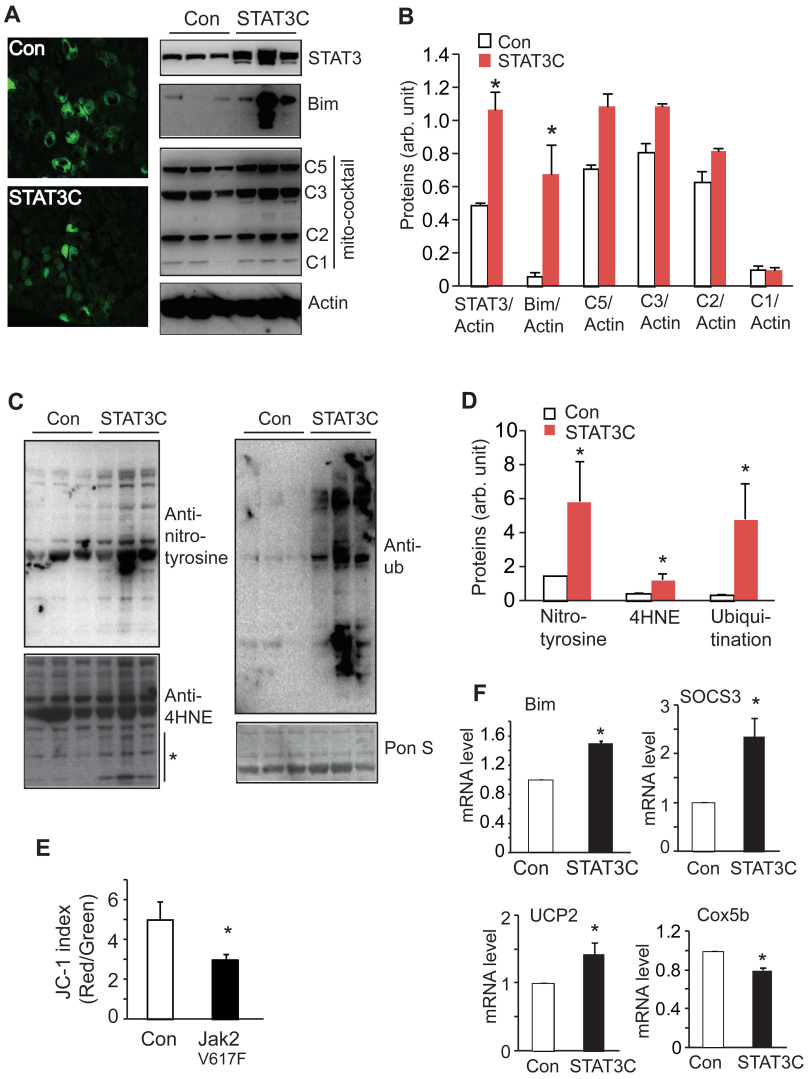

Figure 3. Overexpression of constitutively active STAT3 induces oxidative stress. (A) Constitutively active STAT3 (STAT3C) induces the protein expression of Bim (Bcl2l11), but not the components in electron transportation chain. Twenty microgram of pcDNA3-STAT3C plasmid, together with 2 μg of pcs2GFP plasmid, was electroporated into mouse TA muscle. GFP+ fibers were isolated 10 d later and total protein extracts were subjected to Western blot analysis (n = 3 pairs of mouse muscles). Left pane shows the efficiency of electroporation. Green fibers are those with the GFP expression. Right panel shows the results of Western blot analysis. C1: NDUFB8, C2: DHB, C3: UQCRC2 and C5: ATP5A. (B) Quantitative data of protein expression changes in (A). ImageJ was used for quantitation of gray density on the Western blot (n = 3 pairs, $*p < 0.05$). (C,D) Constitutively active STAT3 (STAT3C) induces protein oxidation and ubiquitination *in vivo*. (C) Samples were prepared as in (A), and Western blot analysis was performed. Ponceau S (Pon S) is shown as loading control. (D) Quantitative data of protein expression changes in (C). ImageJ was used for quantitation of gray density on the Western blot (n = 3 pairs, $*p < 0.05$). (E) Activated JAK2 suppresses mitochondrial membrane potential. Constitutively active JAK2V617F was transfected into HEK293 cells for 3 d, followed by JC-1 assay. JC-1 index is the ratio of aggregated JC-1 over monomeric JC-1 (n = 6, $*p < 0.05$). (F) Activated STAT3 (STAT3C) alters the expression of genes involved in regulating mitochondrial function. Plasmid expressing constitutively active STAT3C was transfected into HEK293 cells for 3 d. Total RNA was collected and quantitative PCR was performed to examine the mRNA levels (n = 4 experimental/control pairs, $*p < 0.05$). Con, control; arb. unit, arbitrary unit.

phosphorylation of JAK2 and STAT3 (Figure 4A). Blocking the activation of JAK–STAT with a JAK inhibitor suppresses the H_2O_2-induced STAT3 phosphorylation/activation (Figure 4B) and consequently reduces the H_2O_2-induced nuclear enrichment of STAT3 (Figure 4C). H_2O_2-induced oxidative stress leads to increased protein posttranslational modification through carbonylation (anti-DNP) and nitration (anti-nitrotyrosine). This induction is reduced by either the JAK inhibitors (pan-JAK inhibitor I [JAK I] and R545) or the STAT inhibitor stattic (Figures 4D, E; Supplementary Figure S2). In addition, H_2O_2-induced protein ubiquitination also is blocked by either JAK or STAT inhibitors (see Figures 4D,E, Supplementary Figure S2). Mitochondrial membrane potential and ATP generation are both reduced by H_2O_2-induced oxidative stress, and this reduction is attenuated by pretreatment with either the JAK or STAT inhibitor (Figures 4F, G).

These data demonstrate that H_2O_2-induced oxidative stress activates the JAK–STAT signaling pathway, and, conversely, that the JAK–STAT pathway is important in the development of H_2O_2-induced oxidative stress. These observations suggest that activation of JAK–STAT by ROS might facilitate the development of a vicious cycle during MV.

DISCUSSION

Prolonged dependence upon MV is an enormous problem in our hospitals' intensive care units. As the duration of MV rises, so does the incidence of complications such as ventilator-associated pneumonia (53). The longer the period of full ventilator support, the more severe VIDD becomes (20), creating a downward spiral that may become irreversible and even result in death. An enormous cost in both lives and health system dollars is thus incurred by the problem of VIDD. Prevention of VIDD would be likely to have a major impact upon the morbidity, mortality and costs of intensive care medicine.

We report here that the posttranslational activation of JAK–STAT in a MV

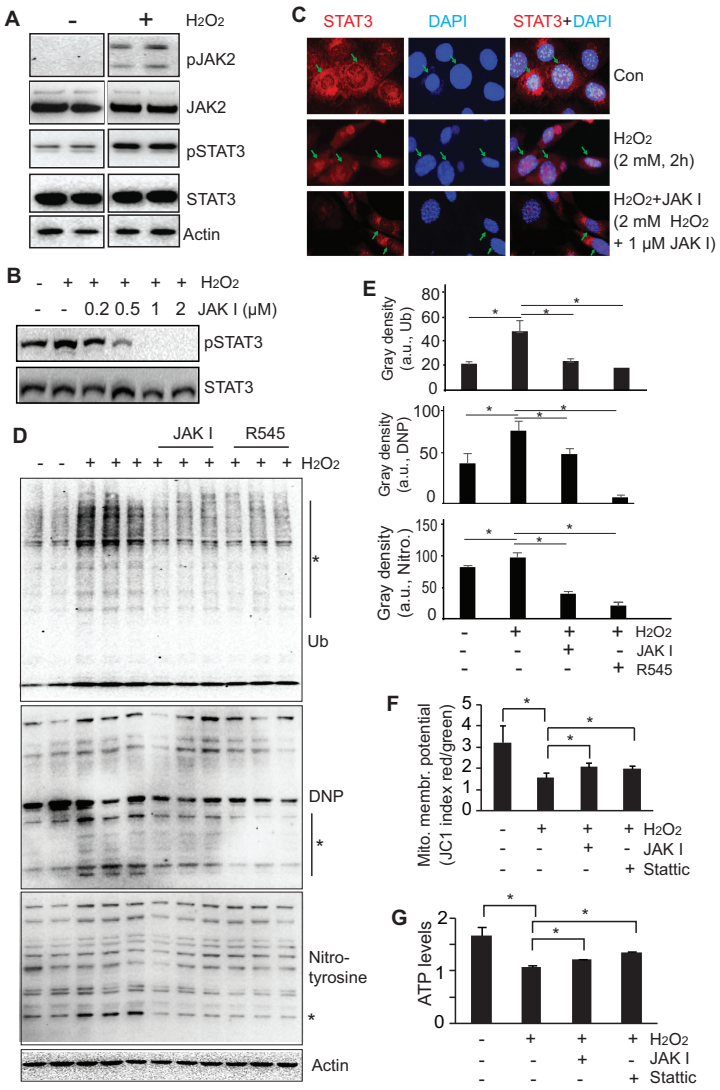

Figure 4. JAK–STAT is activated by H_2O_2 and is required for H_2O_2-induced oxidative stress. (A) H_2O_2 activates the JAK–STAT pathway by inducing the phosphorylation of JAK2 and STAT3. C2C12 myotubes were treated with H_2O_2 (2 mmol/L) for 2 h and total cell lysates were subjected to Western blot analysis. (B,C) A pan-JAK inhibitor (JAK I) blocks the H_2O_2-induced phosphorylation (B) and nuclear enrichment (C) of STAT3. (B) C2C12 myotubes were treated with H_2O_2 (2 mmol/L) in the presence or absence of JAK I for 2 h, and total cell lysates were subjected to Western blot analysis. (C) Immunostaining was performed on cultured C2C12 cells. C2C12 myotubes were treated with H_2O_2 (2 mmol/L) for 2 h in the presence or absence of JAK I. STAT3 (red) was stained with STAT3 antibody and nuclei were stained by DAPI (blue), green arrows show the location of nuclei. (D) H_2O_2-induced protein posttranslational modifications are reduced by JAK inhibitors. C2C12 myotubes were treated with H_2O_2 (200 μmol/L, 18 h) in the presence or absence of the pan-JAK inhibitor (JAK I, 1 μmol/L) or R545 (0.5 μmol/L). Protein oxidation and nitration were examined by antibodies against DNP and nitrotyrosine, and protein ubiquitination was detected by anti-ubiquitin antibody. (E) Quantitation of the modified proteins. The gray density of the indicated areas (*) in (D) were quantitated. *$p < 0.05$. (F,G) The reduction in mitochondrial membrane potential and ATP production with H_2O_2 treatment is reversed by JAK and STAT inhibitors. C2C12 myotubes were treated with H_2O_2 (200 μmol/L, 18 h) in the presence or absence of pan-JAK inhibitor (JAK I, 0.2, 0.5 μmol/L) and STAT inhibitor (stattic; 0.2, 0.5 μmol/L) (n = 6, *$p < 0.05$). Con, control; Ub, ubiquitin; Nitro., nitrotyrosine; a.u., arbitrary unit.

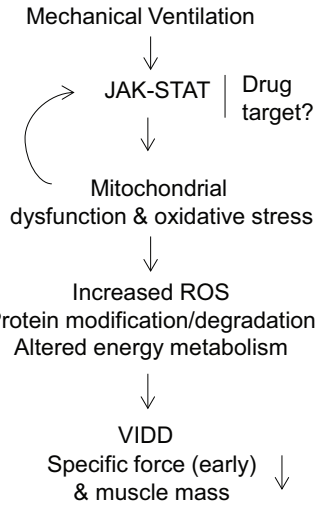

Figure 5. Schematic of the proposed role of JAK–STAT in the pathogenesis of ventilator-induced diaphragm dysfunction (VIDD).

diaphragm is directly linked to reductions in diaphragm muscle contractility. In both mechanically ventilated human and rat diaphragms, the JAK–STAT pathway is significantly activated. We show that activated JAK–STAT results in oxidative stress and mitochondrial dysfunction, and that inhibition of JAK–STAT prevents this oxidative stress and the reduction in diaphragm muscle contractility. Therefore, a drug that inhibits JAK–STAT administered early in a patient's intensive care unit stay, may be able to prevent VIDD (Figure 5).

In addition to being the first demonstration of the activation of JAK–STAT in MV human diaphragm tissue, the current study goes beyond a previous publication concerning the JAK–STAT pathway in VIDD (51) by elucidating the underlying mechanism by which JAK–STAT increases oxidative stress. We observe that the altered expression of STAT3-regulated genes, such as Bim, UCP and Cox5a, impacts mitochondrial function via reducing membrane potential and/or reducing the efficiency of ATP generation. We also show that the expression of *NDUFS3*, a gene that encodes a core subunit of the mitochondrial membrane respiratory chain (complex I), is suppressed by MV but recovered with JAK inhibitor treat-

ment. This transcriptional regulation is consistent with the fact that the nuclear localization of the transcriptional factor STAT3 increases following phosphorylation at tyrosine 705 (STAT3-Y705) (48). In addition to the effect via STAT-regulated genes, STAT3 may also directly alter mitochondrial function by associating with components of the mitochondrial respiratory chain. This effect is regulated by another phosphorylation site on STAT3, the serine 727 (51,54,55).

Oxidative stress may reduce the specific force of skeletal muscle in several ways, which have been previously reviewed (39–42), including alteration of myofilament structure, cross-bridge kinetics, calcium sensitivity and energy supply. Activated STAT3 has been suggested to regulate energy metabolism by suppressing mitochondrial function in cancer cells (52). In the current study, we observe that STAT3 induces protein oxidation and disables mitochondrial function in muscle cells. It is thus possible that JAK–STAT affects the specific force of diaphragm muscle by both posttranslational modification (for example, ubiquitination, oxidation and nitration) of proteins, as well as by compromising the energy supply. Since protein modifications can occur rapidly and directly affect muscle contractile function, they might account for the rapid occurrence of diaphragm weakness after the institution of MV. The upstream signaling pathways that regulate oxidative stress in muscle cells may thus affect muscle contractility, and herein we provide the detailed evidence that JAK–STAT is an important one of these upstream pathways.

Beyond the functional role of STAT3 in reducing the specific force of diaphragm muscle in MV, our findings also directly link STAT3 activation to atrophy of the muscle fibers via increases in protein ubiquitination. Ventilation-induced diaphragm muscle atrophy is partially blocked by JAK inhibition (51), implying that JAK–STAT also contributes to VIDD via regulation of muscle mass. In addition to the 20S proteasome-mediated degradation of oxidized proteins, STAT3-induced muscle atrophy, like FoxO-induced protein degradation, occurs also through activation of the ATP-dependent 26S ubiquitin-proteasome system (UPS). This observation adds another signaling pathway upstream of muscle atrophy that is additive to the previously reported FoxO-induced protein degradation in VIDD, both of which act through the activation of UPS. JAK–STAT activation, then, plays a central role underlying both of the two changes that constitute the pathogenesis of VIDD, atrophy and intrinsic dysfunction.

Although JAK–STAT is shown here to activate oxidative stress, we also report that oxidative stress is able to activate JAK–STAT in muscle cells *in vitro*. The creation of this apparent vicious cycle suggests that activation of JAK–STAT is likely to be a critical step in the development of oxidative stress in ventilated diaphragm muscle, perhaps underlying the surprisingly rapid evolution of VIDD as compared with, for example, disuse weakness of limb muscle. It is possible that the activation of JAK–STAT by oxidative stress occurs via cytokines, such as interleukins and VEGF, as these factors are induced by H_2O_2 in cultured muscle cells and in ventilated diaphragm (Figure 1, Supplementary Figure S3). It is not surprising that some cytokines/factors are upregulated in diaphragm by mechanical ventilation (24,51; also see Figures 1A–C). What remains to be elucidated is how these secretory cytokines/factors could function locally within diaphragm tissue subjected to MV without causing systemic (for example, nonrespiratory muscle) atrophy. It will be worth exploring whether blocking or neutralizing these cytokines with competitive compounds or antibodies would ameliorate VIDD.

Finally, we have demonstrated the effectiveness of a JAK inhibitor, R545, in preventing MV-induced diaphragm weakness, which indicates the critical role of the JAK–STAT pathway in the development of VIDD. R545 is a nominally selective JAK1/3 inhibitor based on an *in vitro* cell-based assay, but it retains a potent inhibitory effect on JAK2 (Supplementary Table S1). When the compound is delivered into a rat by continuous infusion at the doses used, it would be very difficult to assert that it only inhibits JAK1/3. In our *in vitro* oxidative stress model, R545 and the pan-JAK inhibitor I (JAK I) appear to work equally well. It remains to be elucidated *in vivo* whether or not a pan-JAK inhibitor will achieve even better recovery of diaphragm muscle dysfunction than the nominally selective JAK 1/3 inhibitors. It would be also interesting in the future to test even more specific JAK inhibitors to investigate their effect.

Our *in vivo* demonstration of the prevention of ventilator-associated diaphragm weakness by JAK inhibition, based upon the described solid understanding of the molecular mechanisms of VIDD, provides strong support for continued development of JAK–STAT–targeted drugs to prevent VIDD in the clinic. Since the reduction in the specific contractile force of the diaphragm occurs at the earliest stage of VIDD, prior to the onset of diaphragm muscle atrophy, it is possible that JAK–STAT inhibitors would have particular value by impacting the first, most clinically important component of the clinical syndrome.

CONCLUSION

We have established that the JAK–STAT signaling pathway is activated in the diaphragm of rats and humans subjected to mechanical ventilation. This posttranslational activation of JAK–STAT leads to a reduction of diaphragm contractility through, at least in part, the induction of mitochondrial oxidative stress. JAK–STAT activation appears to be critical in regulating this oxidative stress and is thereby central to the downstream pathogenesis of clinical VIDD. This finding establishes the molecular basis for the therapeutic promise of JAK–STAT inhibitors in ventilated ICU patients, and it identifies a clear mechanism of action that would favor taking such a drug to clinical trials.

ACKNOWLEDGMENTS

We are grateful to Lawrence Argetsinger (University of Michigan) for providing

JAK2 plasmids for this study. We also thank Bianca Kapoor and Isaac Ghansah, and Kun Wang and Yang Gao (Stanford University); and Kelly M McCaughey and Raniel R Alcantara (Rigel Pharmaceuticals) for technical assistance. This work is supported by a Veterans Administration (VA) Biomedical Laboratory R&D Merit Review grant to JB Shrager, and by the grants from the NIH (TR01 AG047820 and R37 AG023806) and the VA (Biomedical Laboratory R&D and Rehab R&D) Merit Reviews to TA Rando.

DISCLOSURE

IJ Smith, GL Godinez, BK Singh, DG Payan, and TM Kinsella are employees and/or stockholders of Rigel Pharmaceuticals, Inc.

REFERENCES

1. Griffiths RD, Hall JB. (2010) Intensive care unit-acquired weakness. *Crit. Care Med*. 38:779–87.
2. Knisely AS, Leal SM, Singer DB. (1988) Abnormalities of diaphragmatic muscle in neonates with ventilated lungs. *J. Pediatr*. 113:1074–7.
3. Laghi F. (2005) Assessment of respiratory output in mechanically ventilated patients. *Respir. Care Clin. N. Am*. 11:173–99.
4. Liu L, *et al*. (2012) Neuroventilatory efficiency and extubation readiness in critically ill patients. *Crit. Care*. 16:R143.
5. Purro A, *et al*. (2000) Physiologic determinants of ventilator dependence in long-term mechanically ventilated patients. *Am. J. Respir. Crit. Care Med*. 161:1115–23.
6. Vallverdú I, *et al*. (1998) Clinical characteristics, respiratory functional parameters, and outcome of a two-hour T-piece trial in patients weaning from mechanical ventilation. *Am. J. Respir. Crit. Care Med*. 158:1855–62.
7. Cattapan SE, Laghi F, Tobin MJ. (2003) Can diaphragmatic contractility be assessed by airway twitch pressure in mechanically ventilated patients? *Thorax*. 58:58–62.
8. Watson AC, *et al*. (2001) Measurement of twitch transdiaphragmatic, esophageal, and endotracheal tube pressure with bilateral anterolateral magnetic phrenic nerve stimulation in patients in the intensive care unit. *Crit. Care Med*. 29:1325–31.
9. Buscher H, *et al*. (2005) Assessment of diaphragmatic function with cervical magnetic stimulation in critically ill patients. *Anaesth. Intensive Care* 33:483–91.
10. Cader SA, *et al*. (2010) Inspiratory muscle training improves maximal inspiratory pressure and may assist weaning in older intubated patients: a randomised trial. *J. Physiother*. 56:171–7.
11. Carlucci A, *et al*. (2009) Determinants of weaning success in patients with prolonged mechanical ventilation. *Crit. Care*. 13:R97.
12. Laghi F, *et al*. (2003) Is weaning failure caused by low-frequency fatigue of the diaphragm? *Am. J. Respir. Crit. Care Med*. 167:120–7.
13. Martin AD, *et al*. (2002) Use of inspiratory muscle strength training to facilitate ventilator weaning: a series of 10 consecutive patients. *Chest*. 122:192–6.
14. Martin AD, *et al*. (2011) Inspiratory muscle strength training improves weaning outcome in failure to wean patients: a randomized trial. *Crit Care*. 15:R84.
15. Hudson MB, *et al*. (2012) Both high level pressure support ventilation and controlled mechanical ventilation induce diaphragm dysfunction and atrophy. *Crit. Care Med*. 40:1254–60.
16. Powers SK, *et al*. (2013) Ventilator-induced diaphragm dysfunction: cause and effect. *Am. J. Physiol. Regul. Integr. Comp. Physiol*. 305:R464–77.
17. Zhu E, *et al*. (2005) Early effects of mechanical ventilation on isotonic contractile properties and MAF-box gene expression in the diaphragm. *J. Appl. Physiol. (1985)*. 99:747–56.
18. Grosu HB, *et al*. (2012) Diaphragm muscle thinning in patients who are mechanically ventilated. *Chest*. 142:1455–60.
19. Hermans G, *et al*. (2010) Increased duration of mechanical ventilation is associated with decreased diaphragmatic force: a prospective observational study. *Crit. Care*. 14:R127.
20. Jaber S, *et al*. (2011) Rapidly progressive diaphragmatic weakness and injury during mechanical ventilation in humans. *Am. J. Respir. Crit. Care Med*. 183:364–71.
21. Levine S, *et al*. (2008) Rapid disuse atrophy of diaphragm fibers in mechanically ventilated humans. *N. Engl. J. Med*. 358:1327–35.
22. Powers SK, *et al*. (2002) Mechanical ventilation results in progressive contractile dysfunction in the diaphragm. *J. Appl. Physiol. (1985)*. 92:1851–8.
23. Mrozek S, *et al*. (2012) Rapid onset of specific diaphragm weakness in a healthy murine model of ventilator-induced diaphragmatic dysfunction. *Anesthesiology*. 117:560–7.
24. Schellekens WJ, *et al*. (2012) Toll-like receptor 4 signaling in ventilator-induced diaphragm atrophy. *Anesthesiology*. 117:329–38.
25. Tang H, *et al*. (2013) Diaphragm muscle atrophy in the mouse after long-term mechanical ventilation. *Muscle Nerve*. 48:272–8.
26. Capdevila X, *et al*. (2003) Effects of controlled mechanical ventilation on respiratory muscle contractile properties in rabbits. *Intensive Care Med*. 29:103–10.
27. Jung B, *et al*. (2010) Adaptive support ventilation prevents ventilator-induced diaphragmatic dysfunction in piglet: an *in vivo* and *in vitro* study. *Anesthesiology*. 112:1435–43.
28. Agten A, *et al*. (2012) Bortezomib partially protects the rat diaphragm from ventilator-induced diaphragm dysfunction. *Crit. Care Med*. 40:2449–55.
29. DeRuisseau KC, *et al*. (2005) Mechanical ventilation induces alterations of the ubiquitin-proteasome pathway in the diaphragm. *J. Appl. Physiol. (1985)*. 98:1314–21.
30. Levine S, *et al*. (2011) Increased proteolysis, myosin depletion, and atrophic AKT-FOXO signaling in human diaphragm disuse. *Am. J. Respir. Crit. Care Med*. 183:483–90.
31. Hussain SN, *et al*. (2010) Mechanical ventilation-induced diaphragm disuse in humans triggers autophagy. *Am. J. Respir. Crit. Care Med*. 182:1377–86.
32. McClung JM, *et al*. (2007) Caspase-3 regulation of diaphragm myonuclear domain during mechanical ventilation-induced atrophy. *Am. J. Respir. Crit. Care Med*. 175:150–9.
33. Nelson WB, *et al*. (2012) Cross-talk between the calpain and caspase-3 proteolytic systems in the diaphragm during prolonged mechanical ventilation. *Crit. Care Med*. 40:1857–63.
34. Welvaart WN, *et al*. (2011) Diaphragm muscle fiber function and structure in humans with hemidiaphragm paralysis. *Am. J. Physiol. Lung Cell Mol. Physiol*. 301:L228–35.
35. Tang H, *et al*. (2011) Intrinsic apoptosis in mechanically ventilated human diaphragm: linkage to a novel Fos/FoxO1/Stat3-Bim axis. *FASEB J*. 25:2921–36.
36. Maes K, *et al*. (2007) Leupeptin inhibits ventilator-induced diaphragm dysfunction in rats. *Am. J. Respir. Crit. Care Med*. 175:1134–8.
37. Shanely RA, *et al*. (2002) Mechanical ventilation-induced diaphragmatic atrophy is associated with oxidative injury and increased proteolytic activity. *Am. J. Respir. Crit. Care Med*. 166:1369–74.
38. Whidden MA, *et al*. (2010) Oxidative stress is required for mechanical ventilation-induced protease activation in the diaphragm. *J. Appl. Physiol. (1985)*. 108:1376–82.
39. Powers SK, Jackson MJ. (2008) Exercise-induced oxidative stress: cellular mechanisms and impact on muscle force production. *Physiol. Rev*. 88:1243–76.
40. Reid MB. (2001) Invited Review: redox modulation of skeletal muscle contraction: what we know and what we don't. *J. Appl. Physiol*. (1985). 90:724–31.
41. Reid MB. (2008) Free radicals and muscle fatigue: Of ROS, canaries, and the IOC. *Free Radic. Biol. Med*. 44:169–79.
42. Smith MA, Reid MB. (2006) Redox modulation of contractile function in respiratory and limb skeletal muscle. *Respir. Physiol. Neurobiol*. 151:229–41.
43. Danshina PV, *et al*. (2001) Mildly oxidized glyceraldehyde-3-phosphate dehydrogenase as a possible regulator of glycolysis. *IUBMB Life*. 51:309–14.
44. Tang H, *et al*. (2012) Oxidative stress-responsive microRNA-320 regulates glycolysis in diverse biological systems. *FASEB J*. 26:4710–21.
45. Wu SB, Wei YH. (2012) AMPK-mediated increase of glycolysis as an adaptive response to oxidative stress in human cells: implication of the cell survival in mitochondrial diseases. *Biochim. Biophys. Acta*. 1822:233–47.

46. Kirkinezos IG, Moraes CT. (2001) Reactive oxygen species and mitochondrial diseases. *Semin. Cell Dev. Biol*. 12:449–57.
47. Bonetto A, *et al*. (2012) JAK/STAT3 pathway inhibition blocks skeletal muscle wasting downstream of IL-6 and in experimental cancer cachexia. *Am. J. Physiol. Endocrinol. Metab*. 303:E410–21.
48. Carballo M, *et al*. (1999) Oxidative stress triggers STAT3 tyrosine phosphorylation and nuclear translocation in human lymphocytes. *J. Biol. Chem*. 274:17580–6.
49. Committee for the Update of the Guide for the Care and Use of Laboratory Animals, Institute for Laboratory Animal Research, Division on Earth and Life Studies, National Research Council of the National Academies. (2011) *Guide for the Care and Use of Laboratory Animals*. 8th edition. Washington (DC): National Academies Press.
50. Picard M, *et al*. (2012) Mitochondrial dysfunction and lipid accumulation in the human diaphragm during mechanical ventilation. *Am. J. Respir. Crit. Care Med*. 186:1140–9.
51. Smith IJ, *et al*. (2014) Inhibition of Janus kinase signaling prevents ventilation-induced diaphragm dysfunction. *FASEB J*. 28:2790–803.
52. Demaria M, *et al*. (2010) A STAT3-mediated metabolic switch is involved in tumour transformation and STAT3 addiction. *Aging (Albany NY)*. 2:823–42.
53. Kallet RH. (2011) Patient-ventilator interaction during acute lung injury, and the role of spontaneous breathing: part 1: respiratory muscle function during critical illness. *Respir. Care*. 56:181–9.
54. Wegrzyn J, *et al*. (2009) Function of mitochondrial Stat3 in cellular respiration. *Science*. 323:793–7.
55. Gough DJ, *et al*. (2009) Mitochondrial STAT3 supports Ras-dependent oncogenic transformation. *Science*. 324:1713–6.